1 **Structural basis for potent neutralization of SARS-CoV-2 and role of antibody affinity**

2 **maturation**

3

4 Nicholas K. Hurlburt[1], Yu-Hsin Wan[1], Andrew B. Stuart[1], Junli Feng[1], Andrew T. McGuire[1,2], Leonidas

5 Stamatatos[1,2], Marie Pancera[1,3]

6

7 [1]Fred Hutchinson Cancer Research Center, Vaccines and Infectious Diseases Division, Seattle, WA, USA

8 [2]University of Washington, Department of Global Health, Seattle, WA, USA

9 [3]Vaccine Research Center, National Institutes of Allergy and Infectious Diseases, National Institute of

10 Health, Bethesda, MD, USA

11 Correspondence: mpancera@fredhutch.org

12

13 **Abstract**

14 SARS-CoV-2 is a betacoronavirus virus responsible for the COVID-19 pandemic. Here, we determined the

15 X-ray crystal structure of a potent neutralizing monoclonal antibody, CV30, isolated from a patient

16 infected with SARS-CoV-2, in complex with the receptor binding domain (RBD). The structure reveals

17 CV30's epitope overlaps with the human ACE2 receptor binding site thus providing the structural basis

18 for its neutralization by preventing ACE2 binding.

19

20

21 **Main**

22 COVID-19 was declared a pandemic in March 2020 by the World Health Organization[1]. As of June 11th,

23 2020, there were ~ 7.4 M infections and over 415,000 deaths worldwide[2]. It is caused by a coronavirus

24 of the beta family, named SARS-CoV-2[3], as it is closely related to SARS-CoV[4]. Their genomes share 80%

25 identity and they utilize angiotensin-converting enzyme 2 (ACE2) as receptor for entry[5-11]. Viral entry

26 depends on the SARS-CoV-2 spike glycoprotein, a class I fusion protein comprised of two subunits, S1

27 and S2. S1 mediates ACE2 binding through the receptor binding domain (RBD), while the S2 subunit

28 mediates fusion. Overall the spike shares 76% amino acid sequence homology with SARS[4]. High

29 resolutions structures of the SARS-CoV-2 stabilized spike in the prefusion revealed that the RBD can be

30 seen in a 'up' or 'down' conformation[5,6].It's been shown that some of the neutralizing antibodies bind

31 the RBD in the 'up' conformation similar to when the ACE2 receptor binds[12]. Currently there is no

32 vaccine available to prevent SARS-CoV-2 infection and highly effective therapeutics have not been

33 developed yet either. The host immune response to this new coronavirus is also not well understood.

34 We, and others, sought to characterize the humoral immune response from infected COVID-19

35 patients[12-14]. Recently, we isolated a neutralizing antibody, named CV30, which binds the receptor

36 binding domain (RBD), neutralizes with 0.03 µg/ml and competes binding with ACE2[15]. However, the

37 molecular mechanism by which CV30 blocked ACE2 binding was unknown. Herein, we present the 2.75

38 Å crystal structure of SARS-CoV-2 RBD in complex with the Fab of CV30 (Extended Data Table 1).

39

40 CV30 binds almost exclusively to the concave ACE2 binding epitope (also known as the receptor binding

41 motif (RBM)) of the RBD using all six CDR loops with a total buried surface area of ~1004 Å^2, ~750 Å^2

42 from the heavy chain and ~254 Å^2 from the kappa chain (Fig. 1A). 20 residues from heavy chains and 10

43 residues from the kappa chain interact with the RBD, forming 13 and 2 hydrogen bonds, respectively

44   (Fig. 1C and Extended Data Table 2). There are 29 residues from the RBD that interact with CV30, 19

45   residues with the heavy chain, 7 residues with the light chain, and 3 residues with both (Extended Data

46   Table 2). Of the 29 interacting residues from the SARS-CoV-2 RBD, only 16 are conserved in the SARS-

47   CoV S protein RBD (Fig. 2c), which could explain the lack of cross-reactivity of CV30 to SARS-CoV S[15]. The

48   CV30 heavy chain is minimally mutated with only a two-residue change from the germline and both of

49   these residues (Val27-Ile28) are located in the CDRH1 and form nonpolar interactions with the RBD. We

50   reverted these residues to germline to assess their role. Interestingly, the germline CV30 (glCV30)

51   antibody bound to RBD with ~100-fold lower affinity (407 nM affinity) (Fig 1d and Extended Data Table

52   3) compared to CV30 (3.6 nM[15]) with a very large difference in the off-rate. glCV30 neutralized SARS-

53   CoV-2 with ~500-fold difference with an IC50 of 16.5 vs 0.03 μg/mL for CV30 (Fig. 1e). Val27 forms a

54   weak non-polar interaction with the RBD Asn487 and sits in a pocket formed by CDRH1 and 3. Although

55   it is unclear, Phe27 presents in glCV30 could change the electrostatic environment. The Ile28 sidechain

56   forms non-polar interactions with the RBD Gly476-Ser447, particularly the Cγ atom, which the glCV30

57   Thr would be incapable of making. Thus, minimal affinity maturation of CV30 significantly impacted the

58   ability of this mAb to neutralize SARS-CoV-2.

59

60   CV30 competes with ACE2 for binding to the RBD[15] and we therefore examined the structural

61   mechanism of the receptor blocking by superimposing the SARS-CoV-2 RBD/ACE2 complex (PDB: 6LZG)[9]

62   with the CV30 Fab/RBD complex. The structure of the RBD was used to align the two complexes and

63   showed that CV30 binding did not induce any conformational changes in the RBD from the ACE2-bound

64   complex. The aligned RBD had a RMSD of 0.353 Å over 166 C_α atoms. The structure reveals that the

65   CV30 epitope overlaps almost completely with the ACE2 epitope. A total of 26 residues of the SARS-CoV-

66   2 RBD interact with hACE2, CV30 binds to 19 of these residues (Fig. 2A), indicating that CV30 neutralizes

67   the virus by preventing the binding of ACE2 to RBD by direct steric interactions.

68

69   Recently, the structure of two potent neutralizing anti-RBD antibodies were published, B38 and CB6[12,14].

70   CV30 shares a similar germline heavy chain V-genes but all three have diverse germline kappa V-genes

71   (CV30 is IGKV3-20*01, B38 is IGKV1-9*01, CB6 is IGKV1-39*01, Extended Data Fig. 1). Both CV30 and

72   B38 use IGHV3-53*01 while CB6 uses IGHV3-66*01, which is only one amino acid different than 3-53*01

73   (Val12 which does not make contact with the epitope). CV30 and CB6 each have higher affinities, 3.6 nM

74   and 2.5 nM, respectively, than B38, 70.1 nM[12,14,15]. Differences in affinity translate into differences in

75   neutralization potency (the IC50s for CV30 and CB6 are 0.03 and 0.036 µg/mL, respectively, and that of

76   B38 is 0.177 µg/mL). Interestingly, Thr28 was also mutated from germline to Ile in B38 but Phe27 was

77   not. CB6 lacks both mutations found in CV30. Differences in other regions of the antibody, such as the

78   CDRH3 and light chain are likely responsible for the overall potency all these antibodies (see below). To

79   investigate the binding mechanism of the three antibodies, a superposition of the structures was

80   created. All three bind in a nearly identical manner with the same angle of approach and similar

81   footprints (Fig. 2b). The alignment of the Fv regions of B38 and CB6 to the Fv region of CV30 had a RMSD

82   of 0.240Å over 100 C_α atoms and 0.329Å over 98 C_α atoms, respectively. Mapping the binding

83   interactions of the RBD to each of the antibodies reveals a close overlap in the binding mechanism (Fig.

84   2c-d). The footprint of the heavy chain is nearly identical, as expected from the shared germline V-gene

85   and sequence similarity. CV30 and CB6 both have longer CDRH3 and bind with higher buried surface

86   area, ~263 and ~251 Å^2, respectively, than B38 (~203 Å^2) (Fig. 2d, Extended Data Fig. 1). The large

87   difference is in the light chain. CV30 has the smallest binding interaction at ~254 Å^2, B38 has the largest

88   interaction at ~497 Å^2 and then CB6 at ~354Å^2. One of the more interesting findings was the interaction

89   of Thr56 in the CV30 CDRK2 which reaches across the RBD and interacts Phe486, an interaction that is

90   not found in the other two antibodies (Extended Data Fig. 1).

91

92   In conclusion, our structure indicates that potent neutralizing antibodies against SARS-CoV-2 bind the

93   receptor binding motif in the RBD, overlapping the ACE2 binding site, but recognize residues that are

94   specific for SARS-CoV-2 only, thus explaining the lack of cross neutralization with SARS-CoV. It is

95   noteworthy that potently neutralizing antibodies isolated from multiple individuals use the same or

96   similar VH gene to target their epitope. Additionally, the minimal affinity maturation observed 21 days

97   after infection in the VH gene of CV30 showed ~100-500-fold increase in affinity and neutralization

98   potency, indicating that further affinity maturation may increase potency and potential cross-reactivity.

99   Our studies indicate that the RBD is a promising target for vaccine design and that these potently

100   neutralizing antibodies should be explored as a treatment for COVID-19 infection.

101

102 **Figure legends**
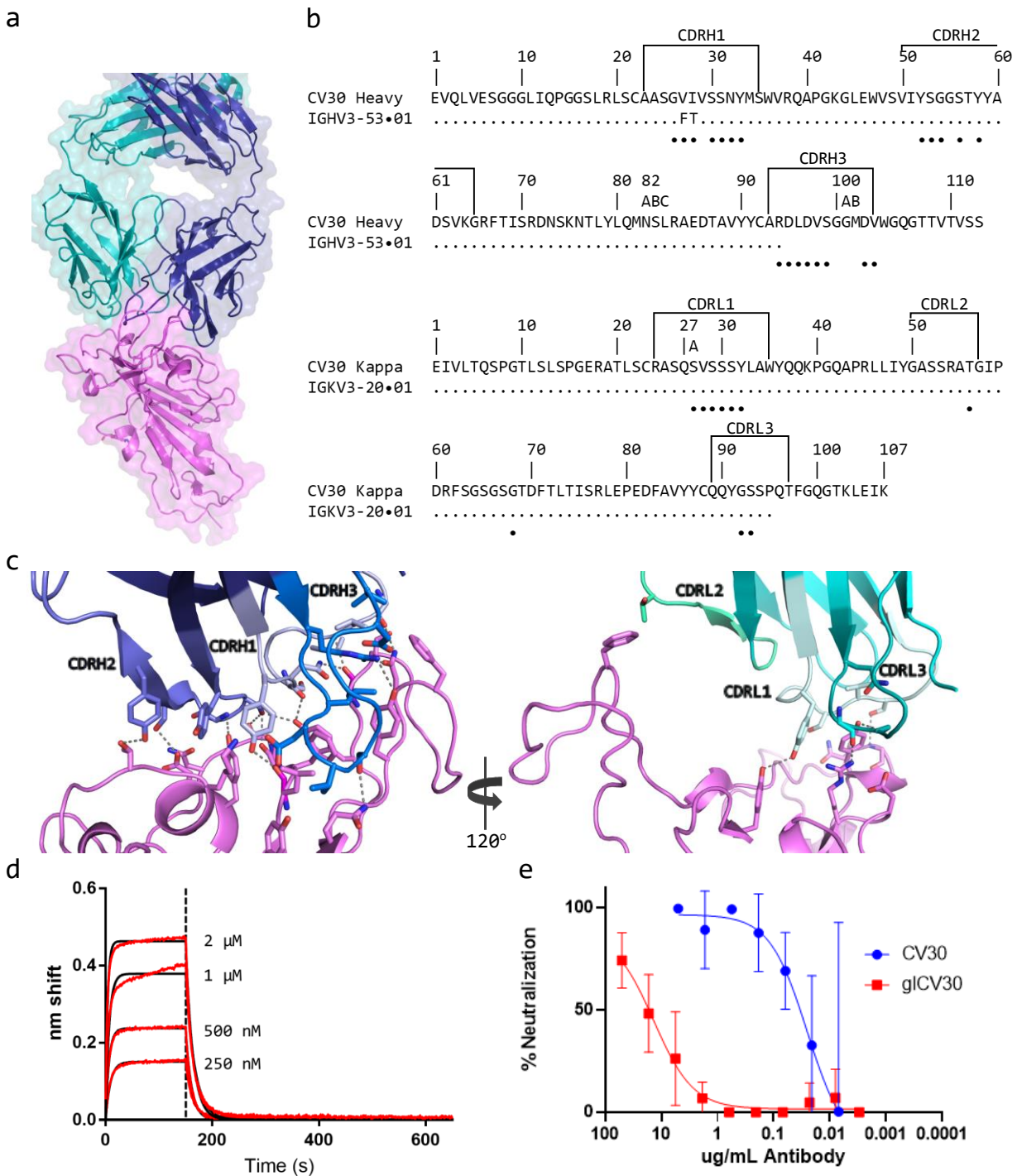
103

104 **Figure 1. Overall structure of CV30 Fab in complex with SARS-CoV-2 RBD and kinetics of glCV30. a.**

105 Structure is shown in cartoon with surface representation shown in transparency. CV30 heavy chain is

106   shown in dark blue and light chain in light blue. RBD is shown in pink. **b.** Sequence alignment of CV30

107   heavy and light chains with germline genes. Black circles underneath the sequence indicate residues that

108   interact with the RBD. **c.** Details of the interactions of the heavy (left) and light (right) chains with the

109   RBD. CDRs are labeled and colored as shown. Residues that interacts are shown as sticks and Hydrogen

110   bonds are shown in dotted lines. **d**. Kinetics of glCV30 binding to RBD measured by BLI. **e**. glCV30 and

111   CV30 neutralization of SARS-CoV-2 pseudovirus.

112
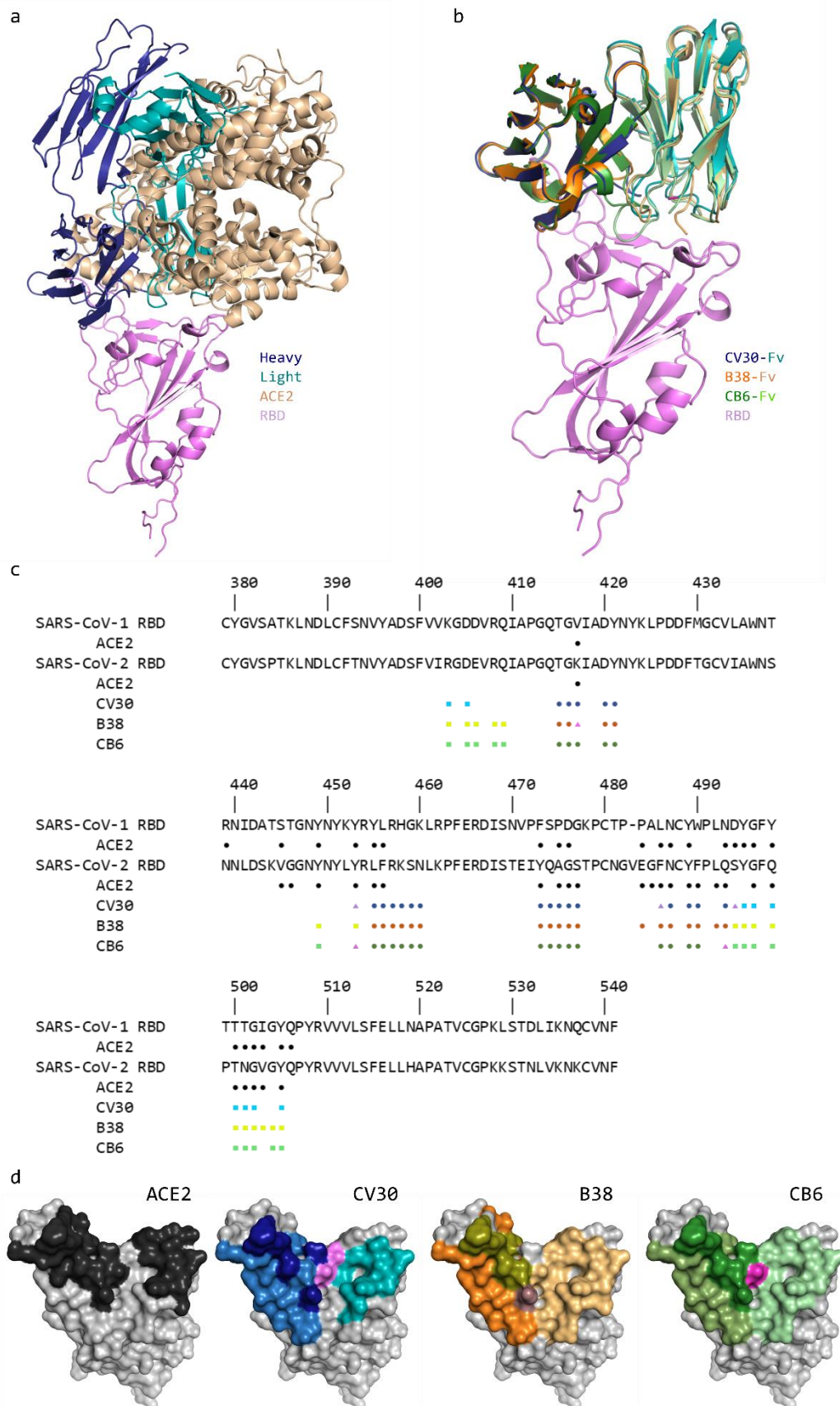
114   **Figure 2. Comparison of the CV30 epitope against ACE2 and other neutralizing antibodies. a**. Structural

115   overlay of ACE2/RBD complex with CV30/RBD complex. **b**. Structural alignment of the variable domains

116   of CV30, B38, and CB6. **c**. Sequence alignment of SARS-CoV RBD and SARS-CoV-2 RBD. The residues that

117   interact with ACE2 are indicated by the black circles. Residues that interact with CV30, B38, and CB6 are

118   indicated by the colored squares (light chain interactions), circles (heavy chain interactions), or triangles

119   (interactions with both chains). **d**. Surface representation of the RBD with the binding epitope colored.

120   Light chain interactions are the lightest color, heavy chain interactions are next lightest, and CDRH3

121   specific interactions are darkest, and interacting with both heavy and light chain is purple.

122

123   **Methods**

124   **Recombinant Protein Expression and Purification**

125   The plasmid encoding the receptor binding domain of SARS-CoV-2 spike protein fused to a monomeric

126   Fc (pαH-RBD-Fc) has been previously described[5] and was a gift from Dr. Jason McLellan.

127   1L of 293SGlycoDelete cells[16] were cultured to a density of 1 million cells/mL and transiently transfected

128   with 500μg of pαH-RBD-Fc using 2 mg of polyethylenimine (PEI, Polysciences, Cat# 24765). Cultural

129   supernatant was harvested 6 days post-transfection by centrifugation and sterile filtered using a 0.22μm

130   vacuum filter. The RBD was purified using protein A agarose resin (GoldBio, Cat# P-400) and cleaving the

131   Fc domain using HRV3C protease (made in house) on-column. The eluate containing the RBD was further

132   purified by SEC using a HiLoad 16/600 Superdex 200 pg column (GE Healthcare) column pre-equilibrated

133   in 2mM Tris-HCl, pH 8.0, 200mM NaCl. Protein was aliquoted, flash frozen, and stored at -80°C until

134   needed.

135

136   500mL of 293EBNA cells were cultured to a density of 1 million cells/mL and transiently transfected with

137   125µg each of CV30 Heavy and Kappa chains using 1 mg of PEI. Cultural supernatant was harvested 6

138   days post-transfection by centrifugation and sterile filtered using a 0.22µm vacuum filter. IgG was

139   purified using protein A agarose resin and eluted using Pierce IgG Elution Buffer (Thermo Scientific, Cat#

140   21004). Eluate was pH adjusted to 7.5 using 1M HEPES, pH 7.5. IgG was further purified by SEC using a

141   HiLoad 16/600 Superdex 200 pg column. Antigen binding fragment (Fab) was generated by incubating

142   IgG with LysC (New England Biolabs, Cat# P8109S) at a ratio of 1µg LysC per 10mg IgG at 37°C for 18hrs.

143   Fab unexpectedly stuck to protein A resin and was eluted as mixture of Fab, undigested IgG, and

144   digested Fc product using the IgG elution buffer. Fab and Fc product was purified by SEC. The CV30-Fab

145   and SARS-CoV-2 RBD complex was obtained my mixing Fab and Fc product with a 2-fold molar excess of

146   RBD and incubated for 90min at RT with nutation followed by SEC. The complex was verified by SDS-

147   PAGE analysis.

148

149   **Crystal Screening and Structure Determination**

150   The complex was concentrated to 10mg/mL for initial crystal screening by sitting-drop vapor-diffusion in

151   the MCSG Suite (Anatrace) using a NT8 drop setter (Formulatrix). Diffracting crystals were obtained in a

152   mother liquor (ML) containing 0.2M (NH$_4$) Citrate, tribasic, pH 7.0 and 12% (w/v) PEG 3350. The crystals

153   were cryoprotected by soaking in ML supplemented with 30% (v/v) ethylene glycol. Diffraction data was

154   collected at Advanced Photon Source (APS) SBC 19-ID at a 12.662 keV. The data set was processed using

155   XDS[17] to a resolution of 2.75Å. The structure of the complex was solved by molecular replacement using

156   Phaser[18] with a search model of SARS-CoV-2 RBD (PDBid: 6lzg)[9] and the Fab structure (PDBid: 5i1e)[19]

157   divided into Fv and Fc portions. Remaining model building was completed using COOT[20] and refinement

158   was performed in Phenix[21]. The data collection and refinement statistics are summarized in Extended

159   Data Table 1. Structural figures were made in Pymol.

160   **BLI**

161   For kinetic analyses glCV30 was captured on anti-Human IgG Fc capture (AHC) sensors at a

162   concentration of 20 µg/mL and loaded for 100s. After loading, the baseline signal was then recorded for

163   1min in KB. The sensors were immersed into wells containing serial dilutions of purified SARS-CoV-2 RBD

164   in KB for 150s (association phase), followed by immersion in KB for an additional 600s (dissociation

165   phase). The background signal from each analyte-containing well was measured using VRC01 IgG control

166   reference sensors and subtracted from the signal obtained with each corresponding glCV30 loaded

167   sensor. Kinetic analyses were performed at least twice with an independently prepared analyte dilution

168   series. Curve fitting was performed using a 1:1 binding model and the ForteBio data analysis software.

169   Mean kon, koff values were determined by averaging all binding curves that matched the theoretical fit

170   with an R2 value of ≥0.98.

171   **Neutralization Assay**

172   HIV-1 derived viral particles were pseudotyped with full length wildtype SARS-CoV-2 S[22]. Briefly,

173   plasmids expressing the HIV-1 Gag and pol (pHDM540 Hgpm2), HIV-1Rev (pRC-CMV-rev1b), HIV-1 Tat

174   (pHDM-tat1b), the SARS-CoV-2 spike (pHDM-SARS-CoV-2 Spike) and a luciferase/GFP reporter (pHAGE-

175   CMV-Luc2-IRES542 ZsGreen-W) were co-transfected into 293T cells at a 1:1:1:1.6:4.6 ratio using 293

176   Free transfection reagent according to the manufacturer's instructions. 72 hours later the culture

177   supernatant was harvested, clarified by centrifugation and frozen at -80˚C.

178   293 cells stably expressing ACE2 (HEK-293T-hACE2) were seeded at a density of 4×10^3 cells/well in a 100

179   µL volume in 96 well flat bottom tissue culture plates. The next day, CV30 and germline CV30 were

180   serially diluted in 30 µL of cDMEM in 96 well round bottom 27 plates in triplicate. An equal volume of

181   viral supernatant diluted to result in 2×10^5 luciferase units was added to each well and incubated for 60

182   min at 37 ˚C. Meanwhile 50 µL of cDMEM containing 6 µg/mL polybrene was added to each well of

183   293T-ACE2 cells (2 µg/mL final concentration) and incubated for 30 min. The media was aspirated from

184   293T-ACE2 cells and 100 µL of the virus-antibody mixture was added. The plates were incubated at 37˚C

185   for 72 hours. The supernatant was aspirated and replaced with 100 µL of Steadyglo luciferase reagent

186   (Promega). 75 µL was then transferred to an opaque, white bottom plate and read on a Fluorskan

187   Ascent Fluorimeter. Control wells containing virus but no antibody (cells + virus) and no virus or

188   antibody (cells only) were included on each plate.

189   % neutralization for each well was calculated as the RLU of the average of the cells + virus wells, minus

190   test wells (cells +mAb + virus), and dividing this result difference by the average RLU between virus

191   control (cells+ virus) and average RLU between wells containing cells alone, multiplied by 100. The

192   antibody concentration that neutralized 50% of infectivity (IC50) was interpolated from the

193   neutralization curves determined using the log(inhibitor) vs. response -- Variable slope (four

194   parameters) fit using automatic outlier detection in Graphpad Prism Software.

195

196   **Data availability**

197   Coordinates and structure factors for CV30 Fab-SARS-CoV-2 RBD complex have been deposited in the

198   Protein Data Bank (PDB) under the accession code 6XE1.

199

200   **References**

201   1.   Mahase, E. Covid-19: WHO declares pandemic because of "alarming levels" of spread, severity,
202   and inaction. *BMJ* **368**, m1036 (2020).
203   2.   Dong, E., Du, H. & Gardner, L. An interactive web-based dashboard to track COVID-19 in real
204   time. *Lancet Infect Dis* (2020).

205   3.   Wu, Y. et al. SARS-CoV-2 is an appropriate name for the new coronavirus. *Lancet* (2020).
206   4.   Wan, Y., Shang, J., Graham, R., Baric, R.S. & Li, F. Receptor Recognition by the Novel Coronavirus
207   from Wuhan: an Analysis Based on Decade-Long Structural Studies of SARS Coronavirus. *J Virol*
208   **94**(2020).
209   5.   Wrapp, D. et al. Cryo-EM structure of the 2019-nCoV spike in the prefusion conformation.
210   *Science* **367**, 1260-1263 (2020).
211   6.   Walls, A.C. et al. Structure, Function, and Antigenicity of the SARS-CoV-2 Spike Glycoprotein. *Cell*
212   (2020).
213   7.   Hoffmann, M. et al. SARS-CoV-2 Cell Entry Depends on ACE2 and TMPRSS2 and Is Blocked by a
214   Clinically Proven Protease Inhibitor. *Cell* (2020).
215   8.   Yan, R. et al. Structural basis for the recognition of SARS-CoV-2 by full-length human ACE2.
216   *Science* **367**, 1444-1448 (2020).
217   9.   Wang, Q. et al. Structural and Functional Basis of SARS-CoV-2 Entry by Using Human ACE2. *Cell*
218   (2020).
219   10.   Letko, M., Marzi, A. & Munster, V. Functional assessment of cell entry and receptor usage for
220   SARS-CoV-2 and other lineage B betacoronaviruses. *Nat Microbiol* **5**, 562-569 (2020).
221   11.   Ou, X. et al. Characterization of spike glycoprotein of SARS-CoV-2 on virus entry and its immune
222   cross-reactivity with SARS-CoV. *Nat Commun* **11**, 1620 (2020).
223   12.   Shi, R. et al. A human neutralizing antibody targets the receptor binding site of SARS-CoV-2.
224   *Nature* (2020).
225   13.   Ju, B. et al. Human neutralizing antibodies elicited by SARS-CoV-2 infection. *Nature* (2020).
226   14.   Wu, Y. et al. A noncompeting pair of human neutralizing antibodies block COVID-19 virus binding
227   to its receptor ACE2. *Science* (2020).
228   15.   Seydoux, E. et al. Analysis of a SARS-CoV-2 infected individual reveals development of potent
229   neutralizing antibodies to distinct epitopes with limited somatic mutation. *Immunity* (2020).
230   16.   Meuris, L. et al. GlycoDelete engineering of mammalian cells simplifies N-glycosylation of
231   recombinant proteins. *Nat Biotechnol* **32**, 485-9 (2014).
232   17.   Kabsch, W. Xds. *Acta Crystallogr D Biol Crystallogr* **66**, 125-32 (2010).
233   18.   McCoy, A.J. et al. Phaser crystallographic software. *J Appl Crystallogr* **40**, 658-674 (2007).
234   19.   Teplyakov, A. et al. Structural diversity in a human antibody germline library. *MAbs* **8**, 1045-63
235   (2016).
236   20.   Emsley, P. & Cowtan, K. Coot: model-building tools for molecular graphics. *Acta Crystallogr D
237   Biol Crystallogr* **60**, 2126-32 (2004).
238   21.   Adams, P.D. et al. Recent developments in the PHENIX software for automated crystallographic
239   structure determination. *J Synchrotron Radiat* **11**, 53-5 (2004).
240   22.   Crawford, K.H.D. et al. Protocol and Reagents for Pseudotyping Lentiviral Particles with SARS-
241   CoV-2 Spike Protein for Neutralization Assays. *Viruses* **12**(2020).

242

243

244

245

Acknowledgments

Author contribution

N.K.H, A.T.M., L.S and M.P. conceived the project. N.K.H, A.T.M., L.S and M.P designed the experiments. J.F. cloned the plasmids. N.K.H and A.B.S. expressed and purified the proteins. N.K.H. crystallized proteins, collected and processed the diffraction data, and solved the crystal structure. N.K.H and A.J.M. performed kinetic experiments. Y-H. W. and A.J.M performed neutralization assay. N.K.H, A.T.M., L.S and M.P. analyzed and discussed data. N.K.H and M.P. wrote the original manuscript draft. N.K.H, A.T.M., L.S and M.P. reviewed and edited the manuscript.